Appl. Phys. A 79, 309–314 (2004)
DOI: 10.1007/s00339-004-2524-2

Applied Physics A
Materials Science & Processing

C. ALTAVILLA
E. CILIBERTO✉

Decay characterization of glassy pigments: an XPS investigation of smalt paint layers

Dipartimento di Scienze Chimiche, Università di Catania, viale Andrea Doria 6, 95125 Catania, Italy

Received: 23 June 2003/Accepted: 18 December 2003
Published online: 19 May 2004 • © Springer-Verlag 2004

ABSTRACT The identification and characterization of a particular pigment in an art object or in a paint layer is an important step in the history of art and technology. Moreover, the understanding of deterioration mechanisms is an essential prerequisite for diagnostics and restoration. In this work we used X-ray photoelectron spectroscopy (XPS) to study pure smalt (cobalt-based blue pigment) and smalt in a tempera media ('leather-glue'). XPS was used to characterize the pure pigment efficiently and to distinguish it in real paint layers. We also studied smalt in leather-glue samples aged in a climatic chamber to investigate the effects of weathering and pollutant concentration on the deterioration process of this paint system.

PACS 81.05.Kf; 81.70.Jb; 82.80.Pv

1 Introduction

Smalt is a pigment obtained by the grinding down of blue-colored potassium glass. The blue color is due to small but variable amounts of cobalt, added as cobalt oxide during manufacture [1]. The principal sources of cobalt used in the preparation of smalt in Europe since the Middle Ages appear to have been the mineral members of the smaltite family ($[Co, Ni]As_{3-2}$), a group of the diarsenide system of Co and Ni with variable concentrations of Fe(II) [2]. In the seventeenth and eighteenth centuries, erytrite ($[Co, Ni]_3[AsO_4]_2 \cdot 8(H_2O)$) and cobaltite (Co, Fe)AsS may also have been used [1].

The manufacturing process of smalt was as follows: the cobalt ores were roasted and the cobalt oxide (CoO) thereby obtained was melted together with quartz and potash or added to molten glass. When poured into cold water, the blue melt disintegrated into particles and these were then ground in water mills and elutriated [1]. Several authors have suggested that smalt was an invention discovered around 1550 by Christoph Schurer, a Bohemian glass-maker [1]. However, earlier cases of smalt used as a pigment have been found, for example in the frescoes by Domenico Ghirlandaio (1449–1494) in the Church of S. Maria Novella in Florence and in the lunette of the main portal of the Church of S. Maria la Vetere in Militello Val di Catania (Sicily), the portal being dated 1506 [2, 3].

The identification and characterization of a particular pigment in an art object or in a paint layer is an important step in the history of art and technology. Moreover, the understanding of deterioration mechanisms is an essential prerequisite for diagnostics and restoration. When exposed to the atmosphere, the surface of a particular paint layer is subjected to degradation processes. Degradation very often leads to profound changes in the chemical species constituting a painting, thus causing deep-set modifications in the chromatic properties of the paint layer. Since the products formed at the early stage of degradation are in the form of very thin layers (only a few nanometers thick), the analytical techniques usually employed for the characterization of solids, such as X-ray diffraction (XRD) or electron-probe microanalysis (EPMA), cannot be used. In this context, X-ray photoelectron spectroscopy (XPS) is a surface technique with great potential as it is possible to obtain a range of chemical information, examples being elemental analysis and the oxidation state of the surface-area elements with a maximum depth of a few nanometers [4]. It is also possible to study the paint coating in a non-destructive manner. Following XPS analysis, samples may be further used in other tests or simply be replaced in the original work of art.

In this work we used XPS to study pure smalt and smalt layers made with tempera binder, in particular with the so-called 'leather-glue' binder, traditionally obtained by extracting collagen proteins from rabbit furs. In order to investigate the effects of weathering on the deterioration process of these paint systems using pollutant species (SO_2 and NO_2) and UV radiation, three kinds of samples were used: freshly prepared samples; samples that had been aged naturally for two years in the city center of Florence; and samples that underwent aging in a climatic chamber.

2 Experimental

Smalt and leather-glue were purchased from Zecchi (Florence) and the samples were formulated and prepared in the Opificio delle Pietre Dure (Florence) by experts skilled in paint using traditional techniques. All the samples were naturally aged for a period of two years in the museum en-

✉ Fax: +39-095/580138, E-mail: eciliberto@dipchi.unict.it

vironment of the Opificio delle Pietre Dure. Some samples underwent an additional aging period of four weeks during which water condensation in the presence of SO_2 and NO_2 was alternated with short periods of UV (365 nm) exposure to avoid possible biological attacks. The aging process was carried out in an HC 4030 Heraeus Vötsch climatic chamber.

XPS measurements were carried out using a PE-PHI ESCA/SAM 5600 monochromator system spectrometer with an analysis chamber base pressure of 5×10^{-10} Torr. X-ray photoemission measurements were performed using a standard Al K_α ($h\nu = 1486.6$ eV) source. The energy scale of the spectrometer was calibrated with reference to the Ag $3d_{3/2} = 368.3$ eV photoelectron line. Binding energies were calculated with respect to the C 1s ionization at 285.00 eV from adventitious carbon that is generally accepted to be independent of the chemical state of the sample under investigation. Overlapping peaks in XPS spectra were resolved by fitting symmetrical Gauss–Lorenzian (80 : 20) functions. The powdered samples were mechanically applied to an indium foil (10 mm × 3 mm) and then fixed onto the spectrometer holder. The paint-layer samples were removed from the glass substrates by lancet, were loaded onto the holder, and analyzed on both sides, corresponding to interfaces air–film and film–substrate. In all the cases the samples being analyzed were subjected to 12 h of ultra-high vacuum (10^{-7} Torr) in a suitable pre-chamber to reduce degassing processes during the measurement period.

3 Results and discussion

The wide-scan X-ray photoelectron spectrum of the pure smalt sample is shown in Fig. 1. The core-level lines Si 2s, Si 2p, Co 3p, Co 2p, K 2s, K 2p, As 3p, As 3d, and O 1s and the Auger lines Co LMM, As LMM, and O KVV can clearly be seen. The presence of these elements is, thus, an important factor in the discrimination of this pigment from other blue pigments. The arsenic traces derive from ores used during the preparation of cobalt oxide.

Figure 2 shows the XPS spectrum in the binding energy region between 775 and 810 eV. The peaks at binding energies 781.3 eV (FWHM = 3.0 eV) and 797.3 eV are attributed to spin–orbit splitting of the Co 2p photoelectron lines [5].

In our study, a strong satellite structure at 5.6 eV on the higher binding energy side of the main peaks was observed. Studies have previously been carried out on a number of cobalt complexes and compounds [5, 6]. In all these studies, the analysis of Co 2p X-ray photoelectron spectra was made difficult by the fact that cobalt can exist in different coordination geometries and different spin states for the same oxidation state. Intense satellite structures were observed for Co 2p spectra, about 5–6 eV above the Co $2p_{1/2}$ and Co $2p_{3/2}$ transitions in the case of high-spin Co^{2+} ($S = 3/2$) compounds, whereas these satellites were seen to be very weak and located about 10 eV above the core-level lines for compounds containing low-spin diamagnetic Co^{3+} ($S = 0$) [7]. The satellite in-

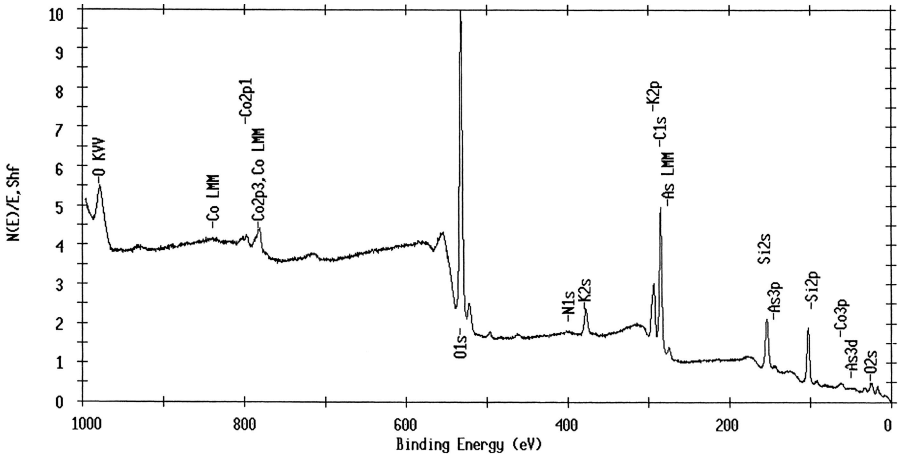

FIGURE 1 XPS wide scan of pure smalt

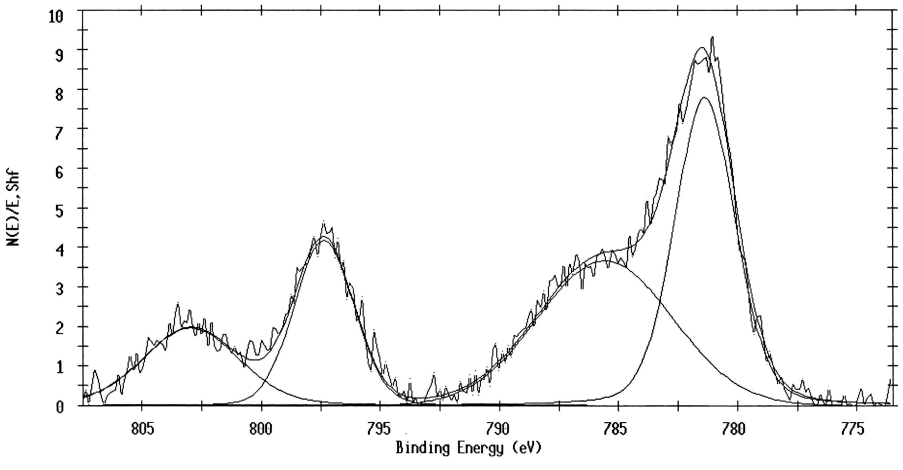

FIGURE 2 XPS Co 2p spectrum for pure smalt

tensities were greater in the high-spin Co^{2+} ($S = 3/2$) than in the low-spin Co^{2+} ($S = 1/2$). This effect was investigated by Briggs and Gibson [6] who reported the binding energy values of various cobalt complexes, observing that the Co $2p_{1/2}$–Co $2p_{3/2}$ spin–orbit splitting increased with the number of unpaired electrons. This increase in the $2p_{1/2}$–$2p_{3/2}$ separation was also observed in nickel(II) complexes [5]. Multiplet splitting in the core level electron binding energy (BE) of paramagnetic species such as Co(II) is, in fact, characteristic of atoms with unpaired orbital spin density where inter-shell exchange interactions operate within the ionic state [8]. In cobalt complexes the $2p_{1/2}$–$2p_{3/2}$ separation was found to be 15.0 eV for diamagnetic Co^{3+}, 15.4 eV for low-spin Co^{2+}, and 16.0 eV for high-spin Co^{2+} [6, 7]. Moreover, Bonnelle and coworkers reported an analysis of the $2p_{1/2}$ core-level transition for CoO, Co_3O_4, and $CoAl_2O_4$ [9, 10]. In the spinel Co_3O_4 they deconvoluted the spectrum of Co $2p_{1/2}$ into two components, one arising from Co^{3+} in the octahedral coordination (oct), and the other from Co^{2+} in the tetrahedral coordination (tet). According to their analysis, the Co^{2+}(tet) shows a binding energy about 1.1 eV higher than the Co^{2+}(oct). This result was also confirmed by the analysis of both $CoAl_2O_4$, in which Co^{2+} is in tetrahedral coordination, and CoO, where Co^{2+} shows an octahedral environment. These studies made it possible to determine the coordination geometry of cobalt as well as the oxidation state and the spin state with great efficiency [8].

In our pure smalt samples, the Co $2p_{1/2}$–Co $2p_{3/2}$ separation is 16.0 eV. Furthermore, strong satellite peaks about 5.6 eV above the main Co 2p lines can clearly be seen (Fig. 2). According to these observations, in the smalt samples cobalt appears to exist both in the Co^{2+} high-spin state ($S = 3/2$) and in a tetrahedral coordination. These results confirm the studies carried out by Bacci and Picollo [11] on similar pigments using fiber optic reflectance spectroscopy in the visible and near-infrared regions.

The O 1s photoelectron core level spectrum is shown in Fig. 3. The spectrum exhibits the main peak at a BE of 532.4 eV with a shoulder at a BE of 530.4 eV. By analogy with sodium silicate glass, it can be asserted that the incorporation of K_2O during manufacture leads to the breaking of tetrahedral Si–O bonds in the glass network [7]. The oxygen atoms linked to two silicon atoms can then generate the signal to a higher BE, while those joined to silicon and potassium ions, the latter being a more electropositive element than silicon, contribute to generate the shoulder at a lower BE (530.4 eV). This component is probably due to the oxygen atoms joined to Co^{2+} also.

An XPS scan of a naturally aged smalt paint layer has been recorded. The interface analyzed is paint layer–air. The N 1s of the protein nitrogen signal is distinctly visible as well as signals generated by smalt (Co 2p, Si 2s, Si 2p, K 2s, and K 2p). Sulphur and other pollutant signals are absent.

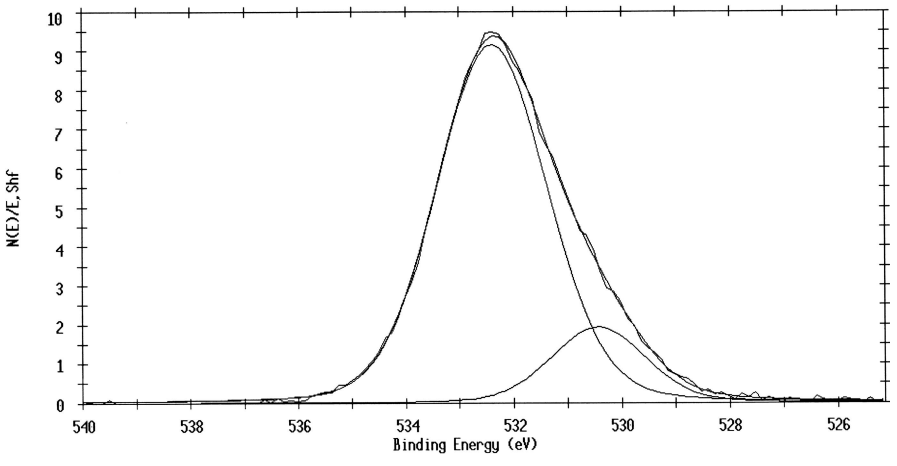

FIGURE 3 XPS O 1s spectrum for pure smalt

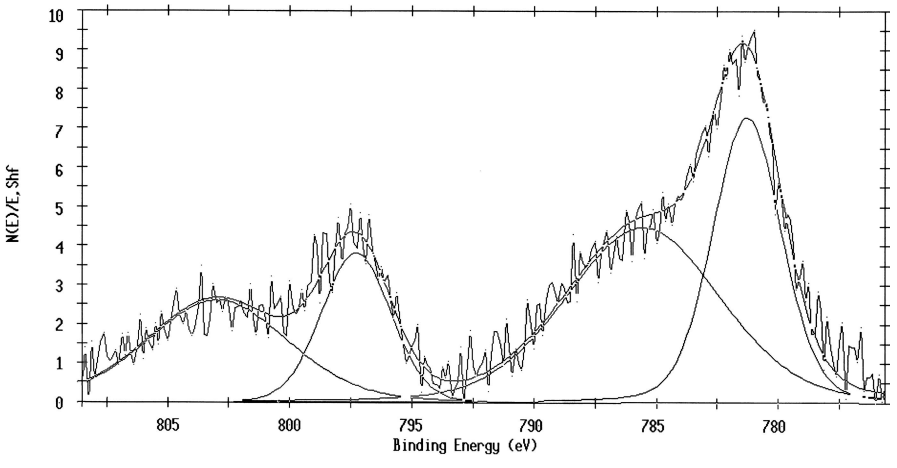

FIGURE 4 XPS Co 2p spectrum for smalt in leather-glue

Co $2p_{3/2}$	Sat. Co $2p_{3/2}$	Co $2p_{1/2}$	Sat. Co $2p_{1/2}$	ΔE $2p_{3/2}$–$2p_{1/2}$
781.3 eV (FWHM 3.3 eV)	785.5 eV	797.3 eV	802.9 eV	16.0 eV

TABLE 1 Binding energies for the Co 2p core-level spectrum and their corresponding satellites. FWHM value is reported in parentheses. ΔE represents the energy separation between Co $2p_{3/2}$ and Co $2p_{1/2}$

Figure 4 shows the Co 2p photoelectron core level spectrum of the sample. Binding energies for the Co 2p doublet core-level spectrum and their corresponding satellites are reported in Table 1.

The N 1s photoelectron core level spectrum is shown in Fig. 5. The signal has a BE of 399.9 eV and shows a little asymmetry at a lower BE (398.9 eV). The position of the peak is typical for protein nitrogen, as fully referred in the literature [12–14]. In fact, 'leather-glue' is a binder essentially made up of collagen, one of the most abundant structure proteins of numerous animal tissues and organs. Furthermore, the spectrum does not show any nitrogen 1s signals arising from nitric and nitrous polluting species.

To evaluate the effects of polluting agents usually present in the air (NO_2 and SO_2), XPS studies were carried out on samples of smalt in leather-glue that had been artificially aged in a climatic chamber as described in Sect. 2.

The aging process has now introduced new signals such as those relating to the sulphur 2s and 2p; the peaks related to Si 2s, Si 2p, Co 2p, and K 2s, produced by pigment; and the N 1s signal produced by the protein binder. It is important to note that the XPS spectrum of the same sample analyzed on the interface film–substrate also shows signals corresponding to ionizations of S 2s and S 2p. Wide spectra are not reported.

The Co 2p photoelectron core-level spectrum is shown in Fig. 6.

In comparison with the naturally aged paint layer, a considerable loss of intensity ($\sim 50\%$) is observed. However, curve fitting made it possible to estimate FWHM values. In particular, for Co $2p_{3/2}$ we observed a 0.6-eV increase in FWHM, a lot greater than the case of a naturally aged film (0.3 eV). This experimental evidence suggests the presence of different cobalt species which cause the broadening of ionization structures. Therefore, artificial aging probably damaged the pigment, stressing a phenomenon that slightly occurred in the paint layers that were aged for two years. Generally, glass is quite a stable material, but it is subjected to deterioration when it interacts with water, aqueous vapor, or pollutant

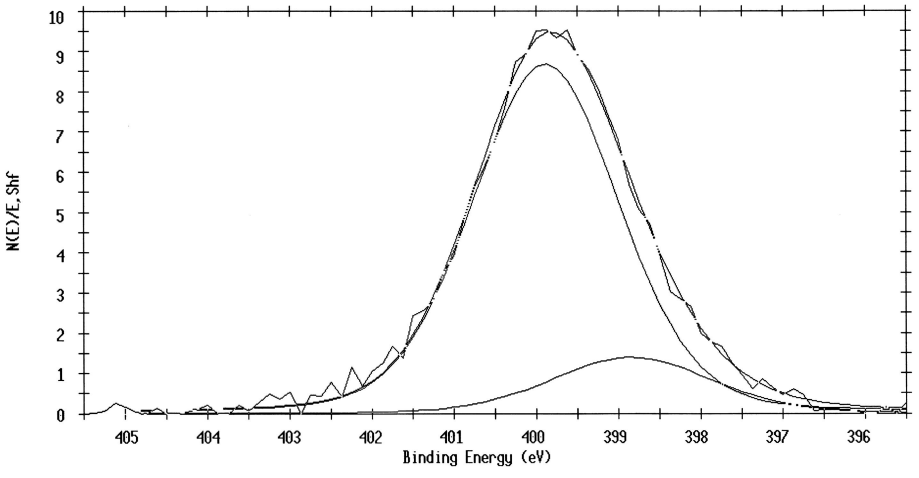

FIGURE 5 XPS N 1s spectrum for smalt in leather-glue

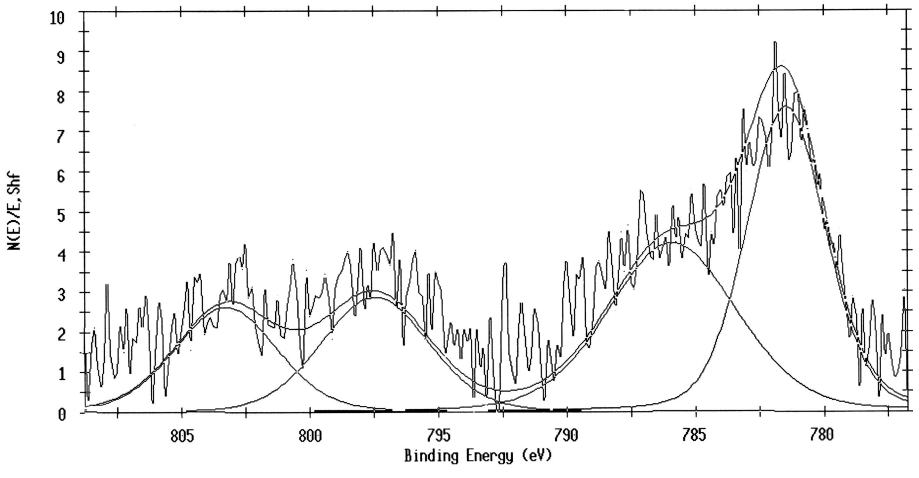

FIGURE 6 XPS spectrum of Co 2p. Smalt in leather-glue artificially aged with SO_2 and NO_2

Smalt in leather-glue	Unaged	Naturally aged for 2 yr	Artificially aged: RH75% 10 ppm NO_x + 1 ppm SO_2	Artificially aged: RH75% 10 ppm NO_x + 10 ppm SO_2
Si/Co	3.5	4.9	8.0	7.8

TABLE 2 Atomic concentration ratios between silicon and cobalt in samples aged in different conditions

species [15, 16]. This phenomenon has been widely observed in many Gothic windows in European cathedrals. Common silicate glasses such as potassium-lime glass or soda-lime glass initially decay via an ionic inter-diffusion process when exposed to water-containing environments. In the ionic inter-diffusion process the alkali ions from the glass exchange and inter-diffuse with hydrogen-bearing ions from water (hydration). The presence of airborne pollutants such as SO_2 and NO_x increases this phenomenon [16]. Smalt (potassium glass) also appears to be subject to this sort of deterioration. Often the alteration is visible to the naked eye as widespread fading. In a previous work, we pointed out micro-exfoliation phenomena in single grains of pigment in a microscopic investigation of Renaissance smalt using Scanning Electro Microscopy-Energy Dispersive X-ray analysis (SEM-EDX), Secondary Ion Mass Spectrometry (SIMS), and XRD techniques [2].

Since the blue color of smalt is due to the presence of high-spin Co^{2+} ions in tetrahedral coordination, the loss of 'color' is probably associated with phenomena of ionic inter-diffusion involving the positive ions present in the glass network. This would explain the significant loss in intensity of the Co 2p XPS signal in the artificially aged paint layer. To quantify this phenomenon, we calculated the atomic concentrations Si/Co % ratio for a group of four paint-layer samples subjected to different aging protocols. The results are set out in Table 2.

The results suggest that the effect of relative humidity (RH) and airborne pollution increases and accelerates the corrosion of smalt, favoring the ionic inter-diffusion process $H^+ \leftrightarrow M^{n+}$ [16] ($M^{n+} = K^+, Co^{2+}$) with a consequent loss of cobalt(II) ions as well as the loss of alkaline ions in the glass network. It is important to note that the simultaneous presence of high concentrations of NO_x and SO_2 does not have a synergistic effect on pigment deterioration. In fact, the ratio between the atomic concentrations of Si/Co remained practically unchanged when different SO_2 concentrations were used during the artificial aging of the paint layers. Cummings and his co-workers reported similar results by analyzing samples of artificially aged soda-lime glass [16]. They measured the hydrogen concentration as a function of depth profile through NRA (nuclear reaction analysis) and the depth profiles of metallic ions through RBS (Rutherford backscattering spectrometry). The results of their studies indicate that environmental pollution with 5 ppm SO_2 and 1 ppm NO_x increases the rate at which glass corrodes by a factor of approximately three in comparison with glass exposed at the same temperature and RH in an ambient of laboratory air.

The S 2p photoelectron core level spectrum is shown in Fig. 7. Curve-fitting analysis shows the presence of a component at 169.5 eV due to sulphur of the sulphate group [17–21] and another component at 167.8 eV that can be attributed to the sulphite species [20, 21]. Previous studies using a variety of investigation techniques carried out on the effects of SO_2 and high RH% [19, 20] on metallic surfaces observed that sulphate and sulphite are the main products on surface samples. When exposure exceeds one day, sulphates are the prevalent species. The same signal with an analogous structure was acquired on the internal surface of our paint-layer sample. This is an important fact, as it constitutes proof that protein binders are permeable to air pollutants and that deterioration involves the paint layer in its entirety.

4 Conclusions

XPS studies carried out on pure smalt and on the smalt in leather-glue made it possible to perform an immediate characterization of the paint layer, discerning pigment identity and the paint technique used to realize the layer with a single analysis. The method used in this study is thus applicable to real painting with unknown compositions. Smalt XPS

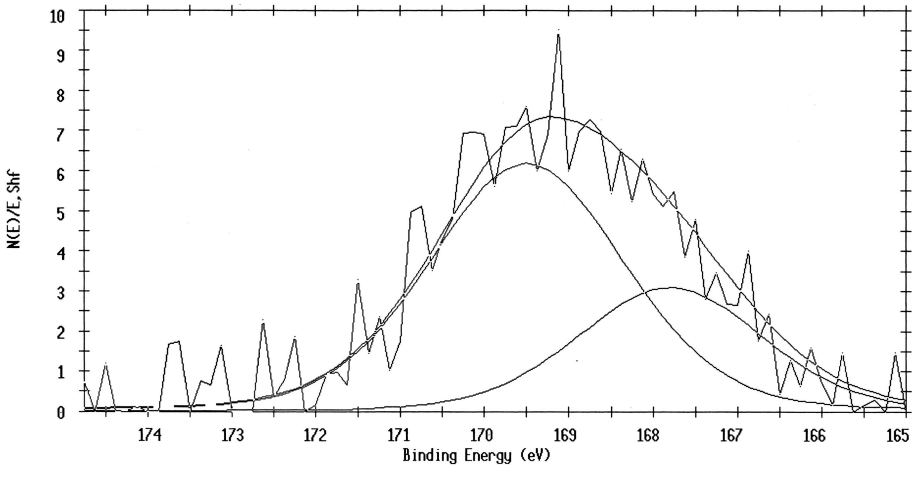

FIGURE 7 XPS spectrum of S 2p. Smalt in artificially aged leather-glue

analysis has confirmed that cobalt in the glass network exists in the high-spin Co^{2+} state ($S = 3/2$) in a tetrahedral coordination and that this is essentially maintained in the naturally aged paint layer. In contrast, the onset of deterioration processes that involve the pigment grains of the paint layer was found in paint models that had been aged in the presence of air pollutants.

An ionic inter-diffusion process involving the surface of pigment grains was also found. This phenomenon causes an increase in the atomic concentration ratio between silicon and cobalt on the surfaces of artificially aged samples. The high humidity content and the presence of SO_2 and NO_x in the reactor atmosphere were seen to increase deterioration, but the simultaneous presence of the two polluting species was not seen to have a synergistic effect on pigment deterioration. Cobalt loss in the glass matrix is thus probably related to the fading that is often visible to the naked eye in old smalt paint layers. The increase of FWHM for Co $2p_{3/2}$, slightly observed for the naturally aged samples and remarkable in models treated with aggressive gases, suggests the partial chemical alteration of cobalt on the surface of the pigment grains. Moreover, the permeability of a paint film toward reactive vapors must be pointed out. This seems to be in agreement with the experimental evidence that tempera paintings are extremely sensitive to polluted environments.

ACKNOWLEDGEMENTS This work has been supported by the Progetto Finalizzato B.C. of Italian Consiglio Nazionale delle Ricerche.

REFERENCES

1 B. Mühlethaler, J. Thissen: Stud. Conserv. **14**, 47 (1969)
2 E. Ciliberto, I. Fragalà, G. Pennisi, G. Spoto: Sci. Technol. Cult. Heritage **3**, 163 (1994)
3 F. Baldini, G. Botticelli, C. Danti, M. Matteini, A. Moles: *Case Studies in the Conservation of Stone and Wall Paintings* (IIC, London, UK 1986)
4 E. Ciliberto, C. Altavilla: LaChim. L'Ind. **7**, 84 (2002)
5 D.C. Frost, C.A. McDowell, I.S. Woolsey: Chem. Phys. Lett. **17**, 320 (1972)
6 D. Briggs, V.A. Gibson: Chem. Phys. Lett. **25**, 493 (1974)
7 A. Mekki, D. Holland, K. Ziq, C.F. McConville: J. Non-Cryst. Solids **220**, 267 (1997)
8 H. Basch: Chem. Phys. Lett. **20**, 233 (1973)
9 J.P. Bonnelle, J. Grimblot, A. D'Huysser: J. Electron Spectrosc. Relat. Phenom. **7**, 151 (1975)
10 J. Grimblot, A. D'Huysser, J.P. Bonnelle, J.P. Beaufils: J. Electron Spectrosc. Relat. Phenom. **6**, 71 (1975)
11 M. Bacci, M. Picollo: Stud. Conserv. **41**, 136 (1996)
12 B. Feng, J. Chen, X. Zhang: Biomaterials **23**, 2499 (2002)
13 D.D. Deligianni, N. Katsala, S. Ladas, D. Sotiropoulou, J. Amedee, Y.F. Missirlis: Biomaterials **22**, 1241 (2001)
14 Y. Tyan, J. Liao, R. Klauser, I. Wu, C. Weng: Biomaterials **23**, 65 (2002)
15 E. Greiner-Wronowa, L. Stoch: J. Non-Cryst. Solids **196**, 118 (1996)
16 K. Cummings, W.A. Lanford, M. Feldmann: Nucl. Instrum. Methods Phys. Res. B **136–138**, 858 (1998)
17 R.V. Siriwardane, J.A. Poston Jr., E.P. Fisher, Ming-Shing Shen, A.L. Milt: Appl. Surf. Sci. **152**, 219 (1999)
18 Y. Limouzin-Maire: Bull. Soc. Chim. Fr. **9–10**, I-342 (1981)
19 J. Itoh, T. Sasaki, T. Ohtsuka, M. Osawa: J. Electroanal. Chem. **473**, 256 (1999)
20 H. Strandberg, L. Johansson: J. Electrochem. Soc. **144**, 81 (1997)
21 M.C. Squarcialupi, G.P. Bernardini, V. Faso, A. Atrei, G. Rovida: J. Cult. Heritage **3**, 199 (2002)